Thermal Flying-Height Control Sliders in Hard Disk Drives

Nan Liu*, Jinglin Zheng and David B. Bogy
Computer Mechanics Laboratory
Department of Mechanical Engineering
5146 Etcheverry Hall
University of California
Berkeley, CA 94720

Abstract

Thermal flying-height control (TFC) sliders are currently used in most commercial hard disk drives (HDDs) as an approach to increase the HDD's capacity and reliability. This paper reviews our recent numerical studies of TFC sliders' flying performances, namely, the heat transfer between the TFC slider and the disk, the flyability of TFC sliders at different altitudes, and the effect of the disk's lubricant and roughness on the TFC slider's flying stability. We validate previous investigations based on a heat transfer model derived from the first order slip theory and identify the instability regimes for a TFC slider flying over a lubricated rough disk.

* To whom correspondence should be made: nanliu@berkeley.edu

1. INTRODUCTION

Hard disk drives (HDDs), the last moving part in state-of-the-art computers, have served as the dominant information storage device for more than five decades. With the introduction of solid state devices (SSDs), HDDs have lost their dominance in the small-capacity storage market such as MP3 players and smart cell phones, but HDDs hold firmly the massive storage market, such as servers and workstations, for which Terabytes of storage capacity is quite common nowadays. To compete with SSDs in the future, the HDDs need to have even larger capacities while maintaining their low cost. Regardless of the approach to achieving this goal, decreasing the distance between the magnetic disk, which is used to store information, and the read-write transducer, which is used to read information from and write information onto the disk, is always required. The theoretical foundation is Wallace's law which states that the strength of reading signal decreases exponentially with the distance between the magnetic disk and the transducer. This distance has been decreasing along with the increase of HDDs' capacity in the last several decades and is now approaching just 5nm. The read-write transducer, made by integrated circuit (IC) technology, is embedded in a slider (less than 1 mm in dimensions) positioned over the magnetic disk rotating to produce linear speeds around 10 – 30 m/s, as shown in Figure 1. The slider is attached to the end of a suspension, which itself is connected to an actuator. When data bits need to be read from or written onto the disk, the voice coil motor (VCM) drives the actuator to move the suspension so that the slider will be positioned over the designated location on the disk.

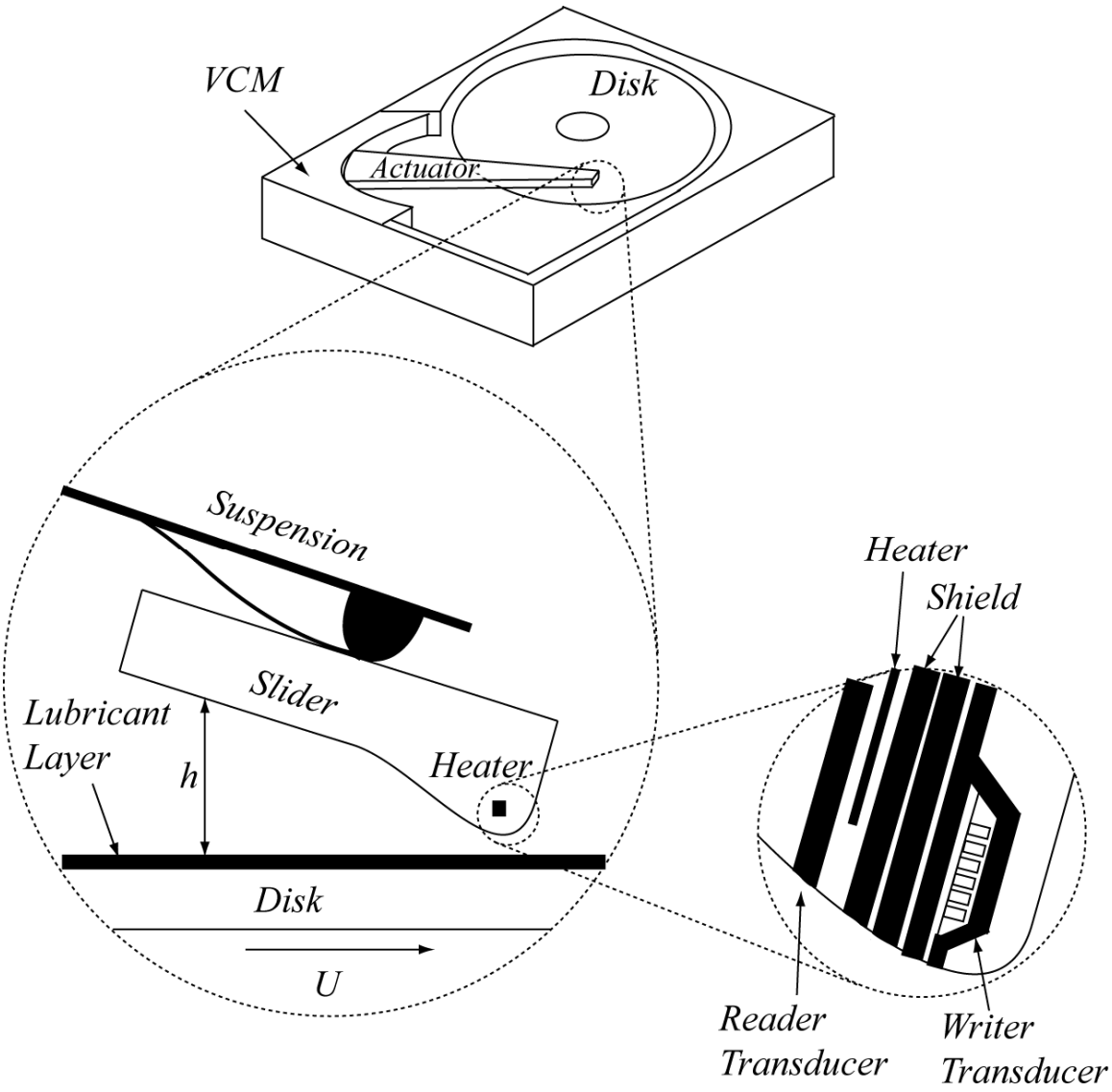

Figure 1 Sketch of a hard disk drive (HDD) and its thermal flying-height control (TFC) slider. The slider is attached to a suspension connected to an actuator. The voice coil motor (VCM) drives the actuator to move the suspension so that the slider can be positioned over a designated location on the disk during a read or write operation. The TFC slider has a heater element embedded in the slider and located near the transducer. When power is applied to the heater element, the slider protrudes locally near the transducer to reduce the distance between the transducer and the disk, which can potentially increase the HDDs' capacity. To reduce potential damage of the disk induced by the impact of the slider, a layer of lubricant (~ 1nm) is put on the top of the disk.

For the HDDs' reliability, the slider needs to fly stably over the disk, i.e., the slider's flying attitude (height, pitch and roll) should change no more than 10 percent when it is

positioned over different locations on the disk. This stable flying attitude is achieved through a careful design of the pattern on the slider's surface facing the disk, known as the air bearing surface (ABS). The rotating disk drags air (due to its viscosity) into the region between the slider and the disk, known as the head-disk interface (HDI), and the air gets compressed and rarefied by the slider's ABS, so that the air pressure on the ABS generates a lift force to balance the load applied by the suspension and keep the slider away from the disk at a designated distance. The state-of-the-art sliders, known as thermal flying-height control (TFC) sliders [1-2], have an embedded heater element near the transducer. The spacing can be at a safe distance but during the HDD's reading or writing operations, power is applied to this heater element and, due to the thermo-mechanical coupling, the slider protrudes locally over a very small area near the transducer so that the distance between the transducer and the disk can be further decreased. Dynamically controllable TFC sliders have been demonstrated, using a feed-forward control approach to make the TFC sliders dynamically compensate the magnetic signal modulation that is associated with disk waviness [3].

The heater element is surrounded by thermal insulators, and additional thermal shields are inserted between the heater and the writer, as shown in Figure 1. This complex structure does not lend itself to analytical studies of the slider's deformation induced by the power applied to the heater, and numerical approaches are instead widely used, which lays the foundation for designs of TFC sliders.

Juang *et al.* [4], and Juang and Bogy [5], proposed an iterative numerical approach, which has now become *de facto*, to calculate the TFC slider's deformation at a given heater power. This approach iterates between two steps: in the first step, the air flow field and the air pressure inside the HDI are obtained by solving a compressible lubrication equation for the particular ABS design and operating parameters; in the second step, the finite element method is used to calculate the slider's deformation induced by the power applied to the heater element with the heat flux and the air pressure on the ABS being boundary conditions.

In Juang *et al.* [4] the slider's deformation induced by the air pressure on the ABS was neglected. This effect was later considered by Juang *et al.* [6] and numerical results for the thermally actuated flying-height as a function of the heater power agrees well with experiments, as presented in Ref. [6].

Based on the iterative approach, Zhang *et al.* [7] studied how the ABS designs affect the TFC slider's performances, such as flying attitude, and found several general guidelines to improve them: reducing the air bearing pressure, reducing the size of the thermo-mechanical actuation area, and decoupling the peak air bearing pressure area from the thermo-mechanical actuation area. Li *et al.* [8] later studied how to design the thermal insulator to improve the TFC sliders' efficiency. They found that reducing the insulator's thermal conductivity and increasing its thickness are helpful. Aoi and Watanabe [9] numerically and experimentally studied how the power applied to the heater element

affects the distance between the transducer and the disk. They found that the relationship between is nonlinear and the distance is mainly affected by the slider's thermal protrusion.

Zhou *et al*. [10] proposed an improved heat transfer model considering the effect of ambient temperature for the calculation of heat flux in the HDI. Based on this model, Zhou *et al*. [11] studied the temperature effect on the TFC slider's flying performances, which, as they found, can be attributed to the temperature dependence of air's viscosity, mean free path and thermal conductivity.

The present paper mainly focuses on numerical investigation of a TFC slider's flying performances and serves as a review of our recent work on this topic. It is organized as follows. In Section II, the theoretical background and the numerical procedure for studying a TFC slider's performance are detailed and the numerical results are compared with experiments. Section III discusses the TFC slider's flying performance at different altitudes that cause different ambient pressures. Section IV discusses a TFC slider flying over a lubricated rough disk (one with root mean square (RMS) surface roughness of about a nanometer). A summary and conclusions are presented in Section V.

2. THEORY AND NUMERICAL PROCEDURE

2.1 Generalized Reynolds Equation

The classical two dimensional Reynolds equation is a reduced Navier-Stokes equation under the condition that the characteristic scale of the air flow channel along one direction is much less than the other two and the Reynolds number of the flow, *Re*, is

much less than 1, where $Re=UL/v$, U is the characteristic speed of the flow, L is the characteristic length of the slider, and v is the kinematic viscosity of the fluid [13-14]. Both of the assumptions hold for the HDI: the air gap thickness, which is everywhere less than a few micrometers, is much less than the slider's length and width, each of which is on the order of millimeter; $Re<<1$ since the disk's linear speed is on the order of 10 – 30 m/s and the air kinematic viscosity is around $10^{-5}m^2/s$.

However, due to the rarefaction of the air (high Knudsen number, where Kn = λ/h, or the mean free path divided by the local spacing), the continuum theory underlying the Navier-Stokes equation does not hold in the entire HDI. A measure of the validity of the continuum theory is the Knudsen number of the flow, which should be less than 0.01 [15-16]. Since mean free path of air at standard conditions is about 65 nm and the air gap thickness in the HDI ranges from a minimum 5nm to around 1μm, the Knudsen number is on the order of 1 to 10. The first attempt to obtain an extended and applicable Reynolds equation was to supplement the Navier-Stokes equation with first order slip boundary conditions on the slider and the disk [17]. But this extension is not sufficient for today's sliders. So along this line, more refined slip boundary conditions were proposed and used to derive extended Reynolds equations [18-22]. Due to the limitation of the constitutive equations used in the Navier-Stokes equations, all the above slip boundary conditions only extend the applicability of the Reynolds equation to a Knudsen number around 0.1 [15-16], which is still too low for its application in the state-of-the-art HDI.

The more accurate approach to describe the flow of a rarefied gas is to use the Boltzmann equation [23-24]. This equation involves a complicated integral of the collisions between molecules, which prohibits analytical studies for most problems. Instead, model Boltzmann equations, which replace the complicated integral with some simple models, are widely used. One model equation, known as the BGK-Boltzmann equation [25], has the benefits of having a simple form and giving results agreeing quantitatively with experiments [23]. Since the characteristic speed of air flow in the HDI, which is on the order of the rotating disk's local linear speed, is much less than the speed of sound in air, the BGK-Boltzmann equation can be linearized. Fukui and Kaneko [26-28] first derived from the linearized BGK-Boltzmann equation a governing equation for the air flow in the HDI and wrote this equation in a form similar to the classical Reynolds equation. This equation is now known as the generalized Boltzmann equation and its dimensionless form is

$$\frac{\partial}{\partial X}\left(Q_p PH^3 \frac{\partial P}{\partial X} - \Lambda_x PH\right) + \frac{\partial}{\partial Y}\left(Q_p PH^3 \frac{\partial P}{\partial Y} - \Lambda_y PH\right) = \sigma \frac{\partial}{\partial T}(PH) \tag{1}$$

where $X= x/L$, $Y =y/L$, x is the distance along the slider's length direction, y is the distance along the slider's width direction, L is the slider's length, $P=p/p_a$, p is the air pressure in the HDI, p_a is the ambient air pressure outside the HDI, $H=h/h_m$, h is the air local gap thickness in the HDI, h_m is a reference air gap thickness, $T=\omega t$, t is time, ω is the disk's angular frequency, $\Lambda_x = 6\mu U_x L / p_a h_m^2$ and $\Lambda_y = 6\mu V_y L / p_a h_m^2$ are the bearing numbers along the x and y directions, U_x and U_y are the disk's speeds along the x and y directions, and Q_p is the dimensionless mass flow rate of the Poiseuille flow part as discussed below.

Equation (1) essentially reflects the conservation of mass. Fukui and Kaneko showed that the total mass flow rate in the HDI is a linear combination of contributions from the Couette flow part and the Poiseuille flow part. They provided a database for calculating the Poiseuille contribution, but use an approximate analytical formula to calculate the Couette part. Kang [29] later introduced a database for the flow rate of the Couette flow part. However, numerical results based on Kang's database are almost identical to those based on Fukui and Kaneko's database [30], and, given its simplicity, Fukui and Kaneko's approach is still widely used. Based on our experiences, the correct implementation of Fukui and Kaneko's database is critical to the successful solution of the generalized Reynolds equation. Thus we employ the original database proposed by them, instead of using some simplified (and thus only agreeing with Fukui and Kaneko's database approximately) databases [31-32] proposed in later publications.

2.2 Heat Transfer in the HDI

The heat transfer between a TFC slider and a disk at different temperatures is difficult to solve, and is not yet fully understood. The first attempt was to solve the continuum Navier-Stokes equation and the energy equation with first order slip boundary conditions for both the velocity and the temperature on the disk and the slider [33-34]. This investigation showed that the heat transfer in the HDI consists of the heat conduction between the slider and the disk due to their different temperatures and the heat dissipation due to the air flow. It also showed that the latter contribution is negligible when compared to the heat conduction part. This finding together with the derived analytical formula for the heat conduction between the slider and the disk at different temperatures

has been widely used as the foundation for calculating the heat transfer between the TFC slider and the disk.

The analytical formula for the heat conduction derived from the first order slip theory happens has the same form as that derived from some approximate method for solving the Boltzmann equation, such as the moment method [35-36], and, to some extent, agrees with experiments and other numerical studies [37]. According to this equation, the heat conduction between the slider and the disk is:

$$q = -k \frac{T_s - T_d}{h + \frac{2-\sigma_T}{\sigma_T} \frac{4\gamma}{\gamma+1} \frac{1}{\mathrm{Pr}} \lambda} \tag{2}$$

where k is the thermal conductivity of air, σ_T is the thermal accommodation coefficient of the ABS, γ is the heat capacity ratio of air, $\mathrm{Pr}=\mu C_p/k$ is the Prandtl number of air, μ is the dynamic viscosity of air, C_p is air's specific heat capacity at constant pressure, λ is the mean free path of air, and T_s and T_d are the slider's and disk's temperature, respectively.

Chen *et al.* [38] compared the heat conduction calculated using Equation (2) with experiments and found that they do not fully agree. In view of the fact that the mean free path used in Equation (2) is defined in a free space without boundaries, they then proposed a remedy by introducing the effect of the presence of the slider and the disk into the calculation of the mean free path. The heat transfer calculated from Chen *et al.*'s [39] formula agrees with both experiments and other widely adopted numerical results.

3.3 Numerical Procedure and Comparison with Experiment

The numerical procedure for studying the TFC sliders' flying performance involves two steps: in the first step, the generalized Reynolds equation is solved by a finite volume method (FVM) to obtain the air flow field and the air pressure field [40]; in the second step, the heat transfer on the slider's ABS is calculated and, together with the air pressure on the ABS, serves as the boundary conditions for the calculation of the slider's thermo-elastic deformation due to the power applied to the heater element [41]. The finite element method (FEM) implemented in a commercial software ANSYS [42] is used in the latter step.

As shown in Figure 2, numerical results based on Equation (1) and those based on Chen *et al*. [38] improved model compare well with experiments with the latter model slightly better. The difference between the predictions from the two models is less than 5% and thus the previous investigation based on the first order slip theory is sufficiently accurate. The agreement with experiments also validates our iterative approach for the investigation of TFC sliders.

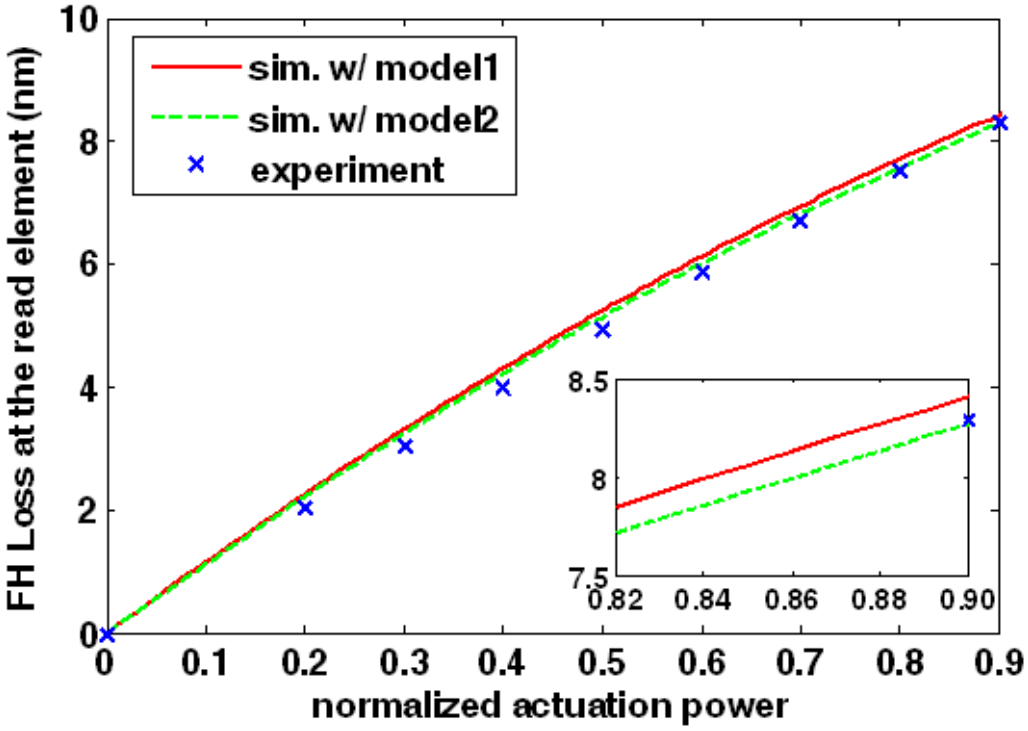

Figure 2 Comparison of numerical prediction and experiments for the flying height loss at the read-write transducer. The flying height loss is defined as the difference between the slider's flying height with the heater turned on and that with the heater turned off. Here model 1 refers to the original model based on the first order slip theory and shown in Equation (2), while model 2 refers to Chen *et al.*'s [38] model with an improved calculation of the mean free path used in Equation (2).

3. EFFECT OF ALTITUDE ON TFC SLIDERS

A TFC slider's performances can be effectively evaluated with use of the iterative approach described in Section 3.3. One useful application is to investigate the effects of ambient conditions on the slider's performances since flying-height fluctuations due to environmental factors (such as pressure drops on airplanes) may result in head-disk contact, and thus damage the read/write transducers. In this case, environmental factors affect the air flow in the head-disk interface, as well as the heat flux across the HDI. This further complicates the coupling between the ABS geometry and the air bearing cooling.

Figure 3 shows the thermally actuated flying-height (FH) for a Femto-sized (0.85×0.70×0.23mm) slider at different heating powers for two altitudes (sea level and 3km) obtained from both simulations and experiments. In simulations, the effects of altitude change is accounted for by modifying the ambient pressure and mean free path used for solving the generalized Reynolds equation and heat flux across the HDI. Experimentally, an altitude chamber is utilized to adjust the ambient pressure. Simulations predict a slightly increased actuated flying-height, which agrees quantitatively with experiments.

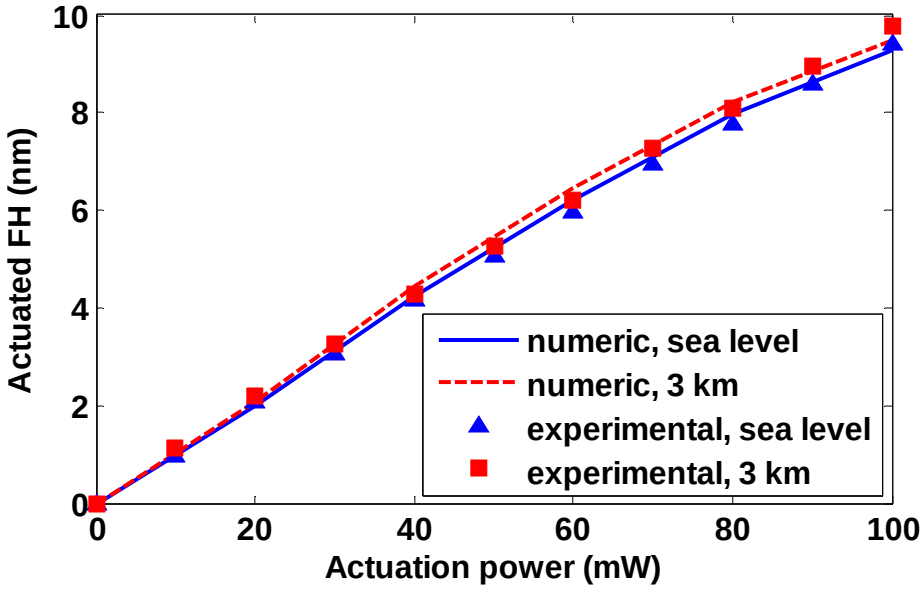

Figure 3 Actuated flying height at different heating powers for sea level and 3 km altitudes. Both simulation and experiment results are included.

Further simulations were conducted to investigate the mechanism of this increased flying-height actuation. The actuated flying-height at the transducer can be written as

$$FH_{actuated} = \alpha \cdot TP \tag{3}$$

where *TP* stands for the thermal protrusion height at the transducer, α is the pushback factor (due to the higher pressure caused by the reduced spacing) at the transducer. Here, *TP* represents the degree of deformation of the air bearing due to the heating, while α shows how much the air flow in the HDI is affected by the localized protrusion and determines what ratio of *TP* finally contributes to the actuated FH.

In Figure 4 we compare the thermal protrusions for three altitudes at the same actuation power. Increased protrusion height is found at the read transducer with increasing altitudes. This can be explained by the kinetics of gas molecules in the HDI. At a higher altitude, the mean free path of air molecules increases, resulting in fewer molecules available in the HDI for energy exchanges. Thus less heat is conducted away from the slider, which leads to the increased local protrusion.

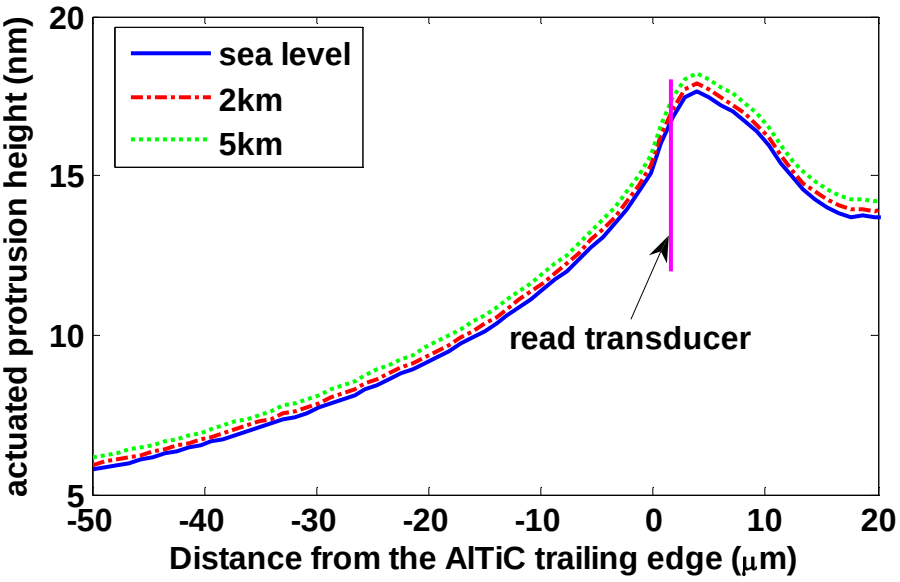

Figure 4 Heater-induced protrusion under a normalized actuation power of 1.0 at three different altitudes: sea level, 2 km and 5km

Figure 5(a) shows a comparison of the pushback factors for the slider flying at sea level and 4km altitudes. Note that the pushback factors can be affected by the ABS geometry. We also simulated the case of the slider with the sea level protrusion but flying at 4km altitude, as shown in Figure 5(a), to exclude the effects due to different protrusion profiles. Pushback factors are lower for the 4km case with the same protrusion profile. With a higher protrusion profile obtained at 4km, the pushback factor is raised, but still lower compared with the sea level case. This can be explained by the air bearing force plot shown in Figure 5(b). By fixing the slider at an attitude of 12 nm flying-height at the trailing edge center, 90 μrad pitch angle and zero roll angle, we obtained the lift forces arising from the air flow in HDI for the same three cases as in Figure 5(a). The sea level case shows a higher rate of change in the air bearing force, which means a stiffer air bearing. In consequence, at a given suspension load, the slider tends to fly higher so that the extra part in the air bearing force can be compensated. Thus, the increased actuated flying-height for TFC sliders at a higher altitude is a composite effect of increased local protrusion and reduced pushback.

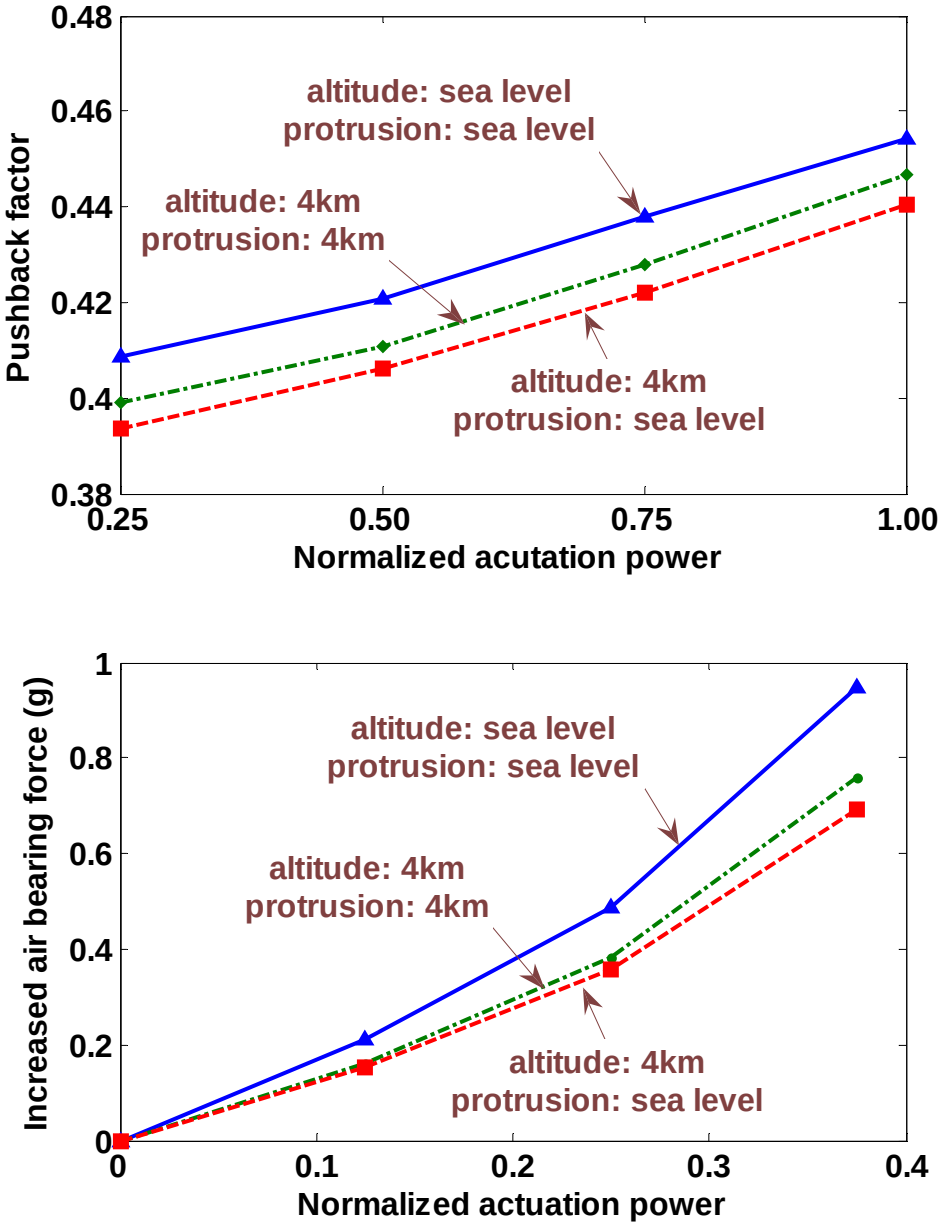

Figure 5 Effect of altitude on the pushback factor (Figure 5a) and on the air bearing force (Figure 5b) for three cases (i) the slider flying at sea level with the protrusion obtained in the sea level case; (ii) the slider flying at 4km with the protrusion obtained in the 4km case; (iii) the slider flying at 4km with the protrusion obtained in the sea level case.

4. EFFECTS OF DISK ROUGHNESS AND LUBRICANT THICKNESS ON A TFC SLIDER'S FLYING STABILITY

Although thermal flying-height control technology provides an effective way of reducing the physical spacing locally, the recording scheme using it for hard disk drives still faces challenges from the increasing demand for higher areal density. Areal density beyond 1 terabits per square inch requires less than 1nm for the physical spacing. At this limit, contact between the slider and disk becomes inevitable.

A surf-recording scheme, which allows contact between the read/write transducer area and the lubricant layer, has been proposed for further reducing the physical spacing while avoiding solid head-disk contact [43]. A major concern associated with this scheme is that the increasing interfacial force between the slider and disk potentially compromises the head-disk interface stability. To explore the feasibility of this scheme, we examine the stability in a process of bringing the slider to touchdown by increasing the thermal protrusion in small increments. At each thermal protrusion step, we solve for the slider's equilibrium flying attitude, and calculate a 3-by-3 stiffness matrix in the form of

$$\begin{bmatrix} \frac{\partial F}{\partial z} & \frac{\partial F}{\partial \theta} & \frac{\partial F}{\partial \varphi} \\ \frac{\partial T_\theta}{\partial z} & \frac{\partial T_\theta}{\partial \theta} & \frac{\partial T_\theta}{\partial \varphi} \\ \frac{\partial T_\varphi}{\partial z} & \frac{\partial T_\varphi}{\partial \theta} & \frac{\partial T_\varphi}{\partial \varphi} \end{bmatrix},$$

where z represents the flying-height coordinate, θ is the pitch angle, φ is the roll angle, F is the total force in the flying-height direction, T_θ is the total pitch torque, and T_φ is the total roll torque. For the obtained equilibrium flying state to be stable, all 3 eigenvalues of this stiffness matrix need to be positive [44]. Otherwise, even if the equilibrium flying-

state exists for the slider, it can not sustain its stability in response to disturbances and, so in the real situation, this can result in an unstable head-disk interface.

For modeling the interfacial forces in the HDI, the most common approach is to combine the analysis based on single-asperity behaviors with assumptions of the asperity geometry and distribution, as was done in Greenwood-Williamson [45]. Assuming isotropic surfaces, the contact load F_c and the adhesion force F_s can be represented as functions of the separation d between two contacting surfaces:

$$F_c = \eta A_n \int_d^\infty \overline{F}_c(u)\phi(u)du \tag{4}$$

$$F_s = \eta A_n \int_{-\infty}^\infty \overline{F}_s(u)\varphi(u)du \tag{5}$$

where η is the areal density of asperities, A_n is the nominal contact area, u is the asperity height as shown in Figure 6, $\phi(u)$ is the asperity height distribution function, and $\overline{F}_c(u)$ and $\overline{F}_s(u)$ are the contact load and the adhesion force for a single asperity.

The presence of a monolayer of lubricant in the head-disk interface complicates the problem. The existence of a liquid in the interface of two solid surfaces may increase the adhesion force, and this is often attributed to the formation of liquid bridges. However, due to the high relative speed between the slider and the disk in HDI, it is difficult to experimentally verify the existence of liquid bridges. Alternatively, Stanley *et al.* [46] developed a sub-boundary lubrication model which is energetically favorable compared with the liquid-bridge scheme, when the lubricant has a strong affinity for the disk overcoat. This model is applied here to account for the adhesion force due to a monolayer

of lubricant. An isotropic surface with asperities having normal-distributed heights and spherical-shaped tips of the same radius R is assumed. By restricting the contact in the elastic range, the adhesion force is further written as

$$F_s = \eta A_n \begin{Bmatrix} \int_{-\infty}^{d-t} \frac{8}{3}\pi R\delta\gamma \left[\left(\frac{\varepsilon}{d-u-t+\varepsilon} \right)^2 - 0.25 \left(\frac{\varepsilon}{d-u-t+\varepsilon} \right)^8 \right] \varphi(u)du \\ +2\pi R\delta\gamma \int_{d-t}^{d} \varphi(u)du \\ +\int_{d}^{\infty} \int_{r_t}^{\infty} \frac{8}{3} \frac{\delta\gamma}{\varepsilon} \left[\left(\frac{\varepsilon}{z-t+\varepsilon} \right)^3 - \left(\frac{\varepsilon}{z-t+\varepsilon} \right)^9 \right] 2\pi r dr \varphi(u)du \end{Bmatrix} \quad (6)$$

where R is the asperity radius, $\delta\gamma$ is the adhesion energy per unit area, ε is the equilibrium intermolecular distance, t is the thickness of the lubricant layer, as shown in Figure 6. The first integration stands for adhesion forces due to non-contacting asperities. The expression for $\overline{F}_s$ is obtained by integrating the attractive pressure derived from the Lennard-Jones potential over a spherical profile. The second integration represents contributions from asperities in the lube-contact status and the $\overline{F}_s$ expression in this case is simplified by assuming it to be equivalent to that of a sphere in point contact with a flat. The third one represents solid-contact adhesion and the $\overline{F}_s$ is expressed using the classical DMT model [47], where z stands for the separation of the solid surfaces at a radius r and is given by:

$$z(r) = \frac{1}{\pi R} \left[a\left(r^2 - a^2\right)^{1/2} - \left(2a^2 - r^2\right) \tan^{-1} \left(\frac{r^2}{a^2} - 1 \right)^{1/2} \right] \quad (7)$$

where $a=(\omega R)^{1/2}$ is the radius of the contact region, $\omega=u-d$ is the interference, as shown in Figure 7. With the elastic range assumption, the contact force F_c can be obtained by the Greenwood-Williamson model, which gives:

$$F_c = \frac{4}{3}\eta A_n E R^{1/2} \int_d^{\infty} (u-d)^{3/2} \phi(u) du \tag{8}$$

where E is the combined elastic modulus of the two rough surfaces.

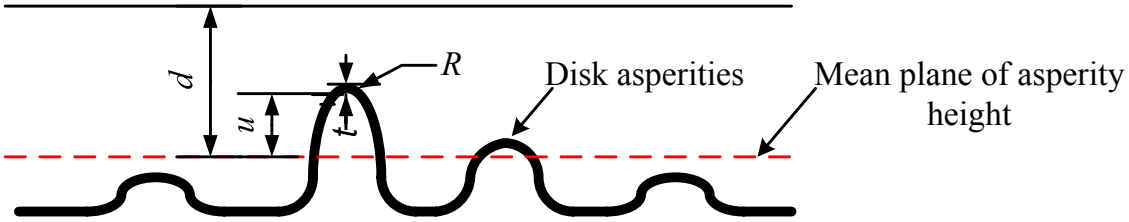

Figure 6 Schematic diagram of slider and disk surfaces not in contact

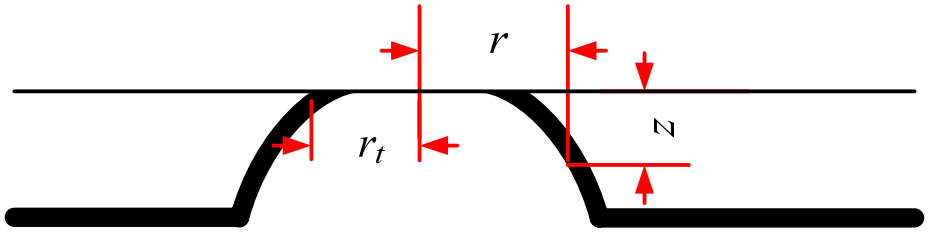

Figure 7 Schematic diagram of an asperity in solid contact with a plane

In the simulation, Equations (6)-(8) are normalized with respect to σ where σ is the standard deviation of the asperity height. F_s and F_c at normalized separations $h=d/\sigma$ are first obtained by numerical integrations and then tabulated in the CML static solver [48] to avoid repeated calculations. For simplicity, the protrusion profile of TFC sliders at each protrusion step is not obtained through the iterative approach described above. Instead, we first obtained a protrusion profile using the iterative approach with 106mW actuation power and take it as a base profile. Increased thermal actuation is then realized by increasing this base profile proportionally.

Three lubricant thicknesses (t=0.8 nm, 1.0 nm, and 1.2 nm) are investigated. The relationship between the minimum separation d^* and the peak thermal protrusion height

is shown in Figure 9, where each point represents an equilibrium state solution obtained by CML static solver. If the stiffness matrix associated with an equilibrium state has negative eigenvalues, it is then marked out by stars. For each lubricant thickness, an instability region exists but over different ranges, which are tabulated in Table 1. In this instability region there is a comparatively steeper drop in the minimum separation d^* with increasing thermal protrusion. Figure 10 shows the interfacial forces at different thermal protrusions for t=1.0nm, where the instability region is also marked out with stars. A rapid growth in the magnitude of the adhesion force is found at this instability region. This means the high rate of change in adhesion force at this flying-height range leads to the loss of HDI stability. Figure 10 also shows the overlap region between the adhesion force curve and the interfacial force curve (a sum of the adhesion force and the contact force), which ends at the branching point where the contact force is no longer insignificant. The growth in contact force, as opposed to the adhesion force, adds up to the air bearing lift, and when this matches the increasing rate of adhesion force, the equilibrium state becomes stable again and the instability region ends.

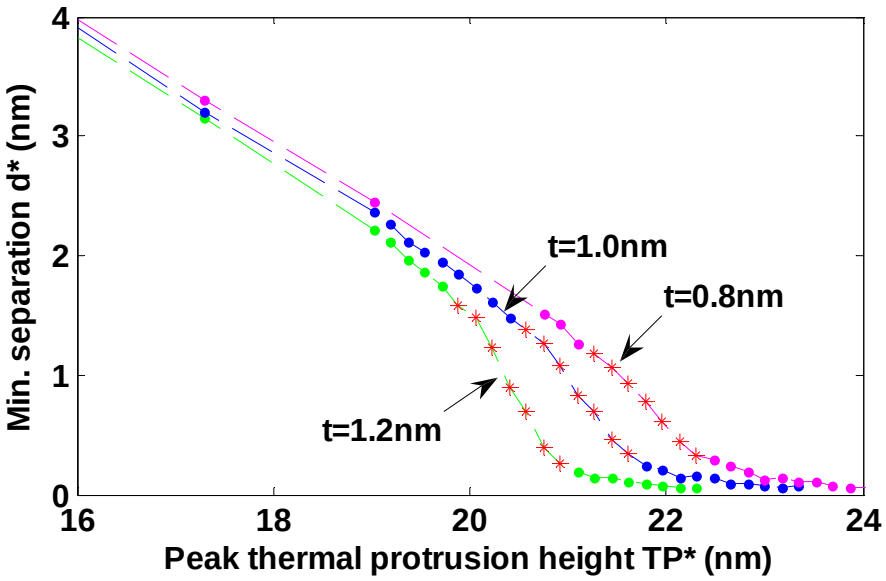

Figure 9 Minimum separation d^* at equilibrium at different thermal protrusions for lubricant thicknesses t=0.8nm, 1.0nm and 1.2nm

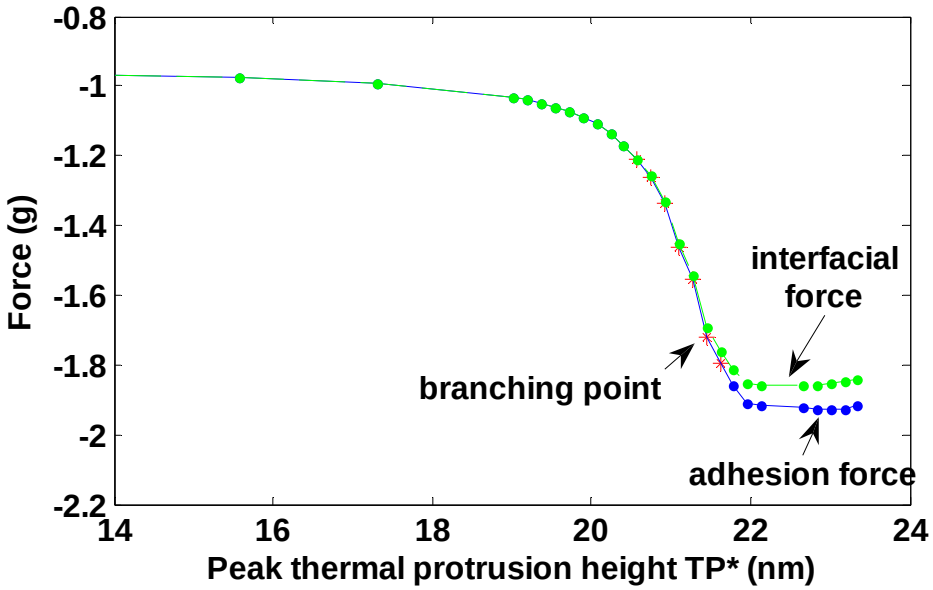

Figure 10 Interfacial forces at equilibrium for different thermal protrusions for t=1.0nm Points with negative stiffness are marked with stars.

Table 1 Extent of the instability regions (IR) for three lubricant thicknesses

Lube Thickness (nm)	d^* at start of IR (nm)	d^* at end of IR (nm)	Extent of IR (nm)
t=0.8	1.180	0.326	0.854
t=1.0	1.385	0.348	1.037
t=1.2	1.586	0.267	1.319

According to Table 1, a thinner lubricant layer results in a lower critical flying-height for the onset of instability, which means the slider can get closer to the disk without losing HDI stability. Thus in the so-called lube-surfing scheme, although the limitations on lube

thickness may be relaxed since slider-lube contact is allowed, such relaxation is quite limited because HDI stability puts another constraint on the lube thickness.

By integrating the probability distribution function of the asperity heights, we get the ratio of asperities as a function of contact status, which is shown in Table 2. For instance, at t=1.0 nm, the slider is stable until the ratio of contacting asperities increases to 30%. Among the 30% contacting asperities only 1% have solid contact. So the slider can be regarded as in a surfing state and it is almost impossible to detect solid contact at this flying state. But at the starred point where the instability region ends, the ratio of contacting asperities grows to 70%, among which 30% are in the solid-contact status. It is quite likely that the solid contact at this flying-state can be detected by such means as acoustic emission transducers placed on the suspension or by read-back signal variation.

Table 2 Contact status at the instability region (IR) for three lubricant thicknesses

	Start of IR		End of IR	
Lube Thickness (nm)	asperities in-contact	Solid-contact asperities	asperities in-contact	Solid-contact asperities
t=0.8	28.1%	3.6%	76.6%	30.9%
t=1.0	27.8%	1.7%	84.1%	29.7%
t=1.2	27.8%	0.7%	92.3%	34.2%

V. Summary and Conclusion

Thermal flying-height control of spacing between the read-write transducer and the disk provides insight into what is required mechanically to increase the capacity of hard disk drives. In this paper, we first proposed an improved model for calculating the heat conduction between the TFC slider and the disk by introducing an approach for the calculation of the mean free path of air in a finite space with boundaries. This improved model gives results in good agreement with experiments. Numerical prediction of the TFC slider's performances based on the original model and the improved one shows little difference and thus validate previous studies based on the original model. We then investigated TFC sliders flying at different altitudes and found that altitude induced changes in the TFC slider's actuated flying height can be attributed to the changes in local protrusion and pushback from the increased air bearing pressure. We also explored the feasibility of the so-called surf-recording scheme with TFC sliders for a storage density beyond 1 terabytes per square inch. An instability region was found to occur with this recording scheme. The lowest achievable stable minimum flying-height in the surf-recording scheme is subject to the existence of this instability region and varies with the lubricant thickness.

Reference

[1] Meyer, D. W., Kupinski, P. E. and Liu, J.C. Slider with temperature responsive transducer positioning. U. S. Patent 5991113, Nov. 23 (1999).

[2] Kurita, M. and Suzuki, K. Flying-height adjustment technologies of magnetic head sliders. IEEE Transaction on Magnetics, 40, 332-336 (2004).

[3] Shiramatsu, T. Atsumi, T., Kurita, M., Shimizu, Y. and Tanaka, H. Dynamically controlled thermal flying-height control slider. IEEE Transaction on Magnetics, 44, 3695-3697 (2008).

[4] Juang, J. Y., Chen, D. and Bogy, D. B. Alternate air bearing slider designs for areal density of 1Tb/in^2. IEEE Transaction on Magnetics, 42, 241-246 (2006).

[5] Juang, J. Y. and Bogy, D. B. Air-bearing effects on actuated thermal pole-tip protrusion for hard disk drives. ASME Journal of Tribology, 129, 570-578 (2007)

[6] Juang, J. Y., Nakamura, T., Knigge, B., Luo, Y. S., Hsiao, W.-C., Kuroki, K., Huang, F.-Y. and Baumgart, P. Numerical and experimental analyses of nanometer-scale flying height control of magnetic head with heating element. IEEE Transaction on Magnetics, 44, 3679-3682 (2008)

[7] Zhang, S., Lee, S.-C., Kim, D., Ferber, J., Strom, B. and Tyndall, G. Air bearing surface designs in consideration of thermo-mechanical actuation efficiency. ASME Journal of Tribology, 130, 041901 (2008).

[8] Li, H., Yin, C.-T. and Talke, F. E. Thermal insulator design for optimizing the efficiency of thermal flying height control sliders. Journal of Applied Physics, 105, 07C122 (2009).

[9] Aoki, K. and Watanabe, T. Nonlinearity of thermal spacing control in hard disk drives. IEEE Transaction on Magnetics, 45, 816-821 (2009).

[10] Zhou, W. D., Liu, B., Yu, S. K., Hua, W. and Wong, C. H. A generalized heat transfer model for thin film bearings at head-disk interface. Applied Physics Letters, 92, 043109 (2008).

[11] Zhou, W. D., Wong, C. H., Liu, B., Yu, S. K. and Hua, W. Effects of temperature dependent air properties on the performances of a thermal actuated slider. Tribology International, 42, 902-910 (2009)

[12] Zhou, W. D., Liu, B., Yu, S. K. and Hua, W. Inert gas filled head-disk interface for future extremely high density magnetic recording. Tribology Letters, 23, 179-186 (2009).

[13] Reynolds, O. On the theory of lubrication and its application to Mr. Beauchamp Tower's experiments, including an experimental determination of the viscosity of olive oil. Philosophical Transactions of the Royal Society of London, 177, 157-234 (1886).

[14] Batchelor, G. K. An Introduction to Fluid Dynamics, Cambridge University Press, Cambridge, 1967

[15] Schaaf, S. A. and Chambré, P. L. Flow of Rarefied Gases, Princeton University Press, Princeton, 1961

[16] Bird, G. A. Molecular Gas Dynamics and the Direction Simulation of Gas Flows, Oxford University Press, New York, 1994

[17] Burgdorfer, A. The influence of the molecular mean free path on the performance of hydrodynamic gas lubricated bearing. ASME Journal of Basic Engineering, 81, 94-100 (1959)

[18] Hsia, Y. T. and Domoto, G. A. An experimental investigation of molecular rarefaction effects in gas lubricated bearings at ultra-low clearances. ASME Journal of Lubrication Technology, 105, 120-130 (1983)

[19] Mitsuya, Y. Modified Reynolds equation for ultra-thin film gas lubrication using 1.5-order slip-flow model and considering surface accommodation coefficient. ASME Journal of Tribology, 115, 289-294 (1993)

[20] Wu, L. and Bogy, D. B. New first and second order slip models for the compressible Reynolds equation. ASME Journal of Tribology, 125, 558-561 (2003)

[21] Shen, S. and Chen, G. A kinetic-theory based first order slip boundary condition for gas flow. Physics of Fluids, 19, 085101 (2007)

[22] Bahukudumbi, P. and Beskok, A. A phenomenological lubrication model for the entire Knudsen number. Journal of Micromechanics and Microengineering, 12, 873-884 (2003)

[23] Cercignani, C. Rarefied Gas Dynamics: From Basic Concepts to Actual Calculations, Cambridge University Press, New York, 2000

[24] Sone Y. Molecular Gas Dynamics: Theory, Techniques, and Applications, Birkhäuser, Boston, 2006

[25] Bhatnagar, P. L., Gross, E. P. and Krook, M. A model for collision processes in gases I: small amplitude processes in charged and in neutral one-component systems. Physical Review, 94, 511-525 (1954)

[26] Fukui, S. and Kaneko, R. Analysis of ultra-thin gas film lubrication based on linearized Boltzmann equation : first report - derivation of a generalized lubrication equation including thermal creep flow. ASME Journal of Tribology, 110, 253-262 (1988)

[27] Fukui, S. and Kaneko, R. Analysis of ultra-thin gas film lubrication based on linearized Boltzmann equation (influence of accommodation coefficient). JSME International Journal, 30, 1660-1666 (1987)

[28] Fukui, S. and Kaneko, R. A database for interpolation of Poiseuille flow-rates for high Knudsen number lubrication problems. ASME Journal Tribology, 112, 78-83 (1990)

[29] Kang, S. C., Crone, R. M. and Jhon, M. S. A new molecular gas lubrication theory suitable for head-disk interface modeling. Journal of Applied Physics, 85, 5594-5596 (1999)

[30] Chen, D. and Bogy, D. B. A comparison of two rarefaction models in the compressible Reynolds equation used in air bearing design for hard disk drives. CML Technical Report 2005-10, Computer Mechanics Laboratory, Department of Mechanical Engineering, University of California, Berkeley, 2005

[31] Shen, C. Use of degenerated Reynolds equation in solving the microchannel flow problem. Physics of Fluids, 17, 046101 (2005)

[32] Wu, L. A slip model for rarefied gas flows at arbitrary Knudsen number. Applied Physics Letters, 93, 253103 (2008)

[33] Zhang, S. and Bogy D. B. A heat transfer model for thermal fluctuation in a thin slider/disk air bearing. International Journal of Heat and Mass Transfer, 42, 1791-1800 (1999)

[34] Chen, L., Bogy, D. B. and Strom, B. Thermal dependence of MR signal on slider flying state. IEEE Transaction on Magnetics, 36, 2486-2489 (2000)

[35] Lees, L. Kinetic theory description of rarefied gas flow. Journal of the society of Industrial and Applied Mathematics, 12, 278-311 (1965)

[36] Vincenti, W. G. and Kruger, C. H. Introduction to Physical Gas Dynamics, Wiley, New York (1965)

[37] Ju, Y. S. Thermal conduction and viscous heating in microscale coquette flow. ASME Journal of Heat transfer, 122, 817-818 (2000)

[38] Chen, D., Liu, N. and Bogy, D. B. A phenomenological heat transfer model for the molecular gas lubrication system in hard disk drives. Journal of Applied Physics, 105, 084303 (2009)

[39] Liu, N. and Bogy, D. B. Predicting the flying height of a thermal flying-height control slider in operation. Submitted to Journal of Applied Physics

[40] Lu, S. Numerical Simulation of Slider Air Bearing, PhD Thesis, Department of Mechanical Engineering, University of California, Berkeley, 1997

[41] Zheng, J. and Bogy, D. B. Thermal fly-height control (TFC) code user's manual. CML Technical Report 2009-06, Computer Mechanics Laboratory, Department of Mechanical Engineering, University of California, Berkeley, 2009

[42] ANSYS 11.0 User's Manual, ANSYS Inc., 2007

[43] Liu, B., Zhang, M. S., Yu, S. K., Hua, W., Ma, Y. S., Zhou, W. D., Gonzaga, L. and Man, Y. J. Lubricant-surfing recording and its feasibility exploration. IEEE Transactions on Magnetics, 45, 899-904 (2009)

[44] Gupta, V. and Bogy, D. B. Dynamics of sub-5nm air bearing sliders in the presence of electrostatic and intermolecular forces at the head disk interface. IEEE Transactions on Magnetics, 41, 610-615 (2005)

[45] Greenwood, J. A. and Williamson, J. B. P. Contact of nominally flat surfaces. Proceedings of the Royal Society of London, A112, 300-319 (1966)

[46] Stanley, H. M., Etsion, I. and Bogy, D. B. Adhesion of contacting rough surfaces in the presence of sub-boundary lubrication. ASME Journal of Tribology, 112, 98-104 (1990)

[47] Muller, V. M., Derjaguin, B.V. and Toporov, Yu. P. On two methods of calculation of the force of sticking of an elastic sphere to a rigid plane. Colloids and Surfaces, 7, 251-259 (1983)

[48] Cox, B. J. and Bogy, D. B. The CML air bearing design program (CMLAir) version 7 user manual. CML Technical Report 2007-13, Computer Mechanics Laboratory, Department of Mechanical Engineering, University of California, Berkeley (2007)